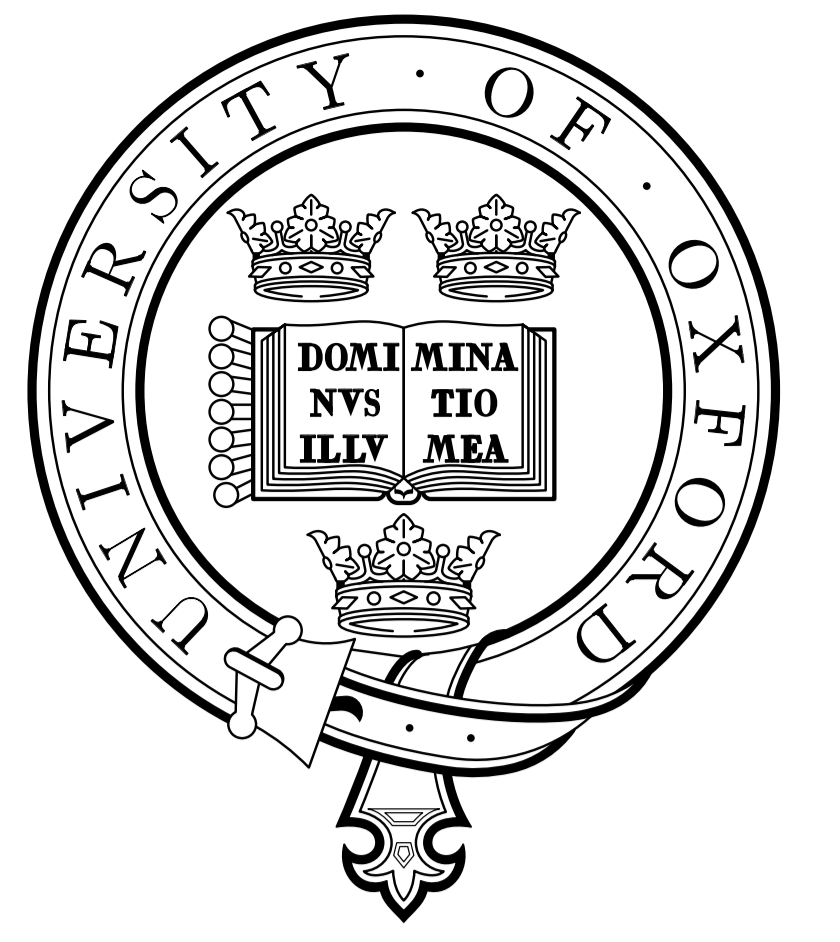


Optical properties of volcanic ash

Dan M. Peters¹, Roy G. Grainger¹, Robert McPheat², Ben Reed¹

[1] University of Oxford [2] Rutherford Appleton laboratory

University of Oxford
Atmospheric, Oceanic and Planetary Physics
Clarendon Laboratory
Parks Road
Oxford OX1 3PU
U.K.
email: dpeters@atm.ox.ac.uk
http://www.atm.ox.ac.uk



1 Abstract

The recent eruption of Eyjafjallajökull volcano has emphasized the importance measuring volcanic ash clouds remotely. Current methods of detection use wavelengths from the UV to infra-red both actively (lidar) and passively (radiometers and spectrometers) on both ground and satellite platforms. Underpinning these remote measurements is the requirement to know the optical properties of the ash. As ash composition varies from eruption to eruption the refractive index also differs; our aim is to derive the refractive index of a range of ashes including Eyjafjallajökull. The refractive index data are required and will underpin remote measurements and further work. This poster shows our latest findings as part of the VANAHEIM project

2 Introduction

Figures 1 and 2 show the illustrate the spectral variation in optical depths for volcanic aerosols. Also show the wavelength channels of AATSR and SEVIRI, in addition MIPAS spectral coverage is shown. Due to the wide spectral range of these channels information on volcanic aerosol speciation exists in the measurements (see Figure 2). Speciation information is contained mainly within the thermal infrared finger-print region. Aerosol size distribution information is contained within the wavelengths in the near infrared.

Limited information exists on ash optical properties. Figure 2 shows the resulting optical depth from the published data. This plot indicates that incorrect choice of optical properties can lead to large errors in remotely retrieved ash properties.

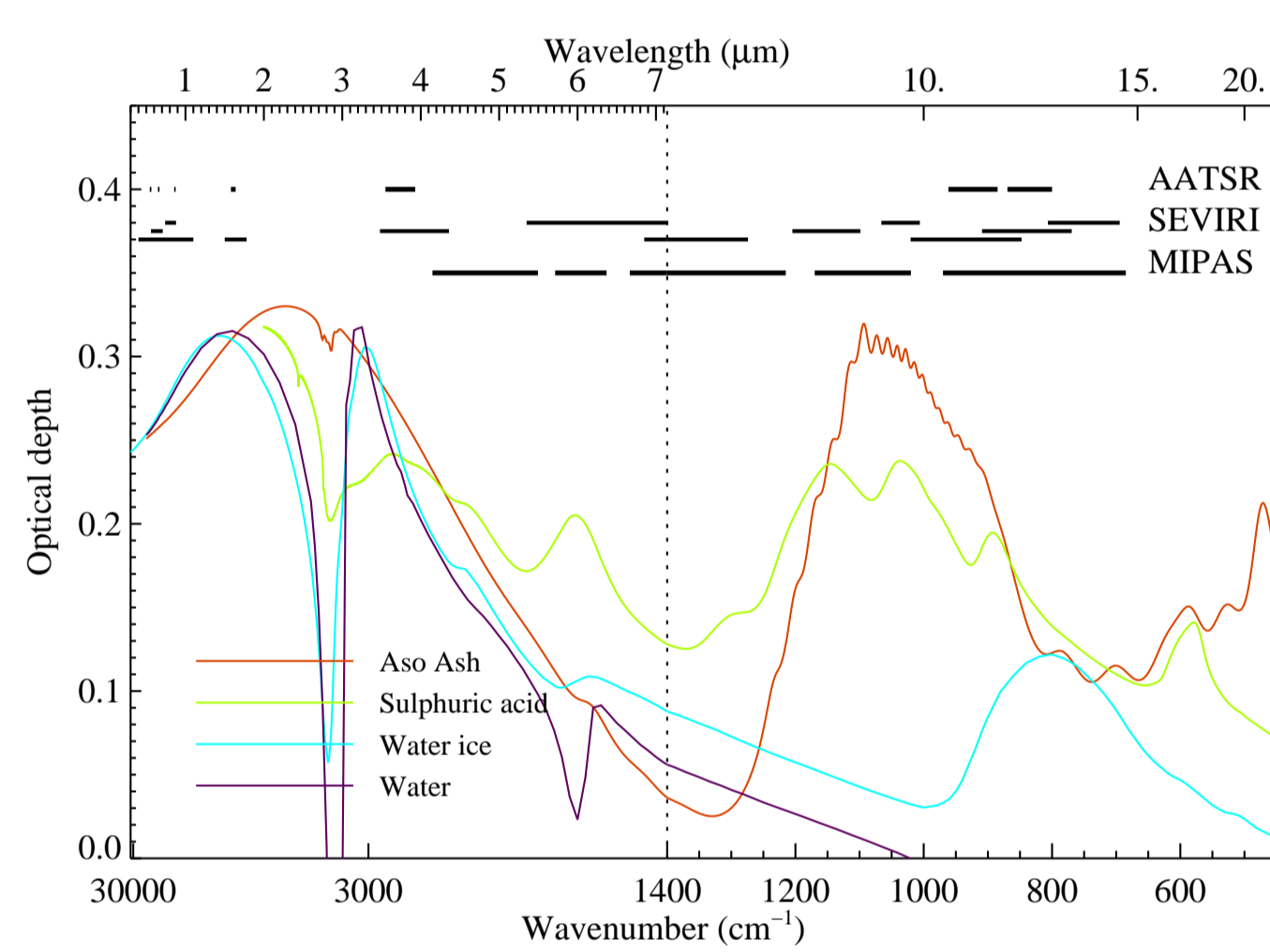


Figure 1: Simulated optical thickness for a 100 m thick plume consisting of a log-normal distribution (number density $2 \times 10^2 \text{ cm}^{-3}$, mode radius $1 \mu\text{m}$, spread 1.7) of spherical particles. The plume is assumed to consist of Aso ash (using the preliminary refractive indices as Figure 7), sulphuric acid (refractive indices from Luo [4]), water ice (refractive indices from Warren [12]) and water (refractive indices from Hale [2]). The black lines at the top of the plot indicate the AATSR and SEVIRI channels and the MIPAS spectral range.

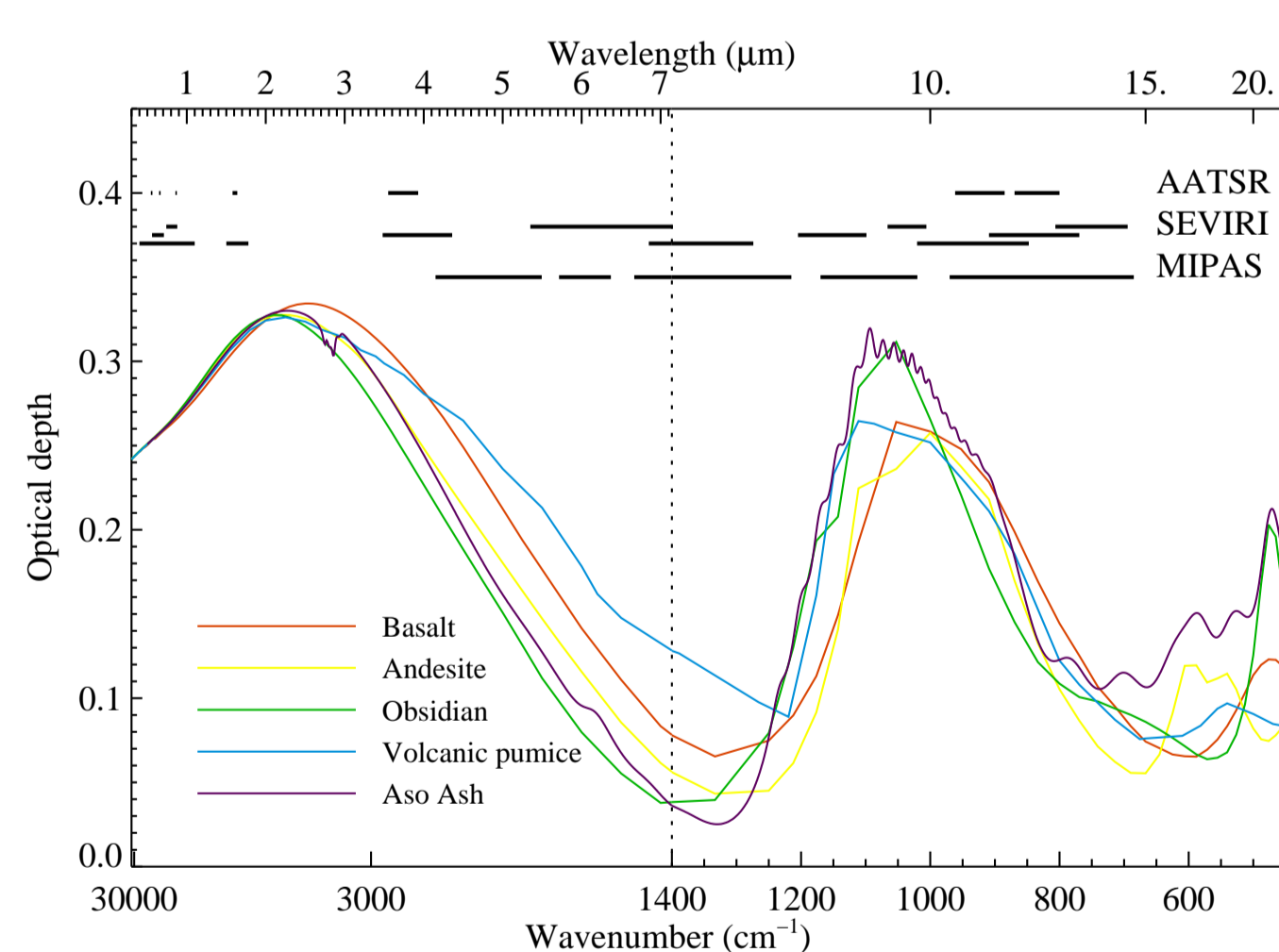


Figure 2: Optical depth different volcanic materials, plotted using same size parameters as Figure 1, but Refractive index data is from, [8] (for basaltic glass, andesite and obsidian) and from Volz, [11] for pumice, see Table 2. The Aso values used the refractive indices given in Figure 7. The black lines at the top of the plot indicate the AATSR and SEVIRI channels and the MIPAS spectral range.

3 Existing published data

Only two published ash infrared refractive index data sets have been found in the literature covering the spectral finger print region (see Table 1, and Figure 3). No data could be found on the real part of the refractive index of ash in the infrared.

Table 1: Limited refractive index data exists on volcanic ashes.

Material	SiO ₂ %wt	Spectral range (μm)	n and k	Reference
Mt. Spur Ash 19/8/1992	50-70	0.34, 0.36, 0.38	n, k	[3]
Mt. St. Hellen's ash	-	0.3-0.7	k	[5]
Mayon ash, andsite	-	1.0-1.6	k	[7]
El Chichón ash (12km, 6/4/1982)	55-61*	0.3-0.7	k	[6]
El Chichón ash (23km, 31/3/1982)	55-61*	0.3-0.7	k	[6]
El Chichón ash (80km, 31/3/1982)	58.77	0.3-0.7	k	[6]

*Only glass component measured

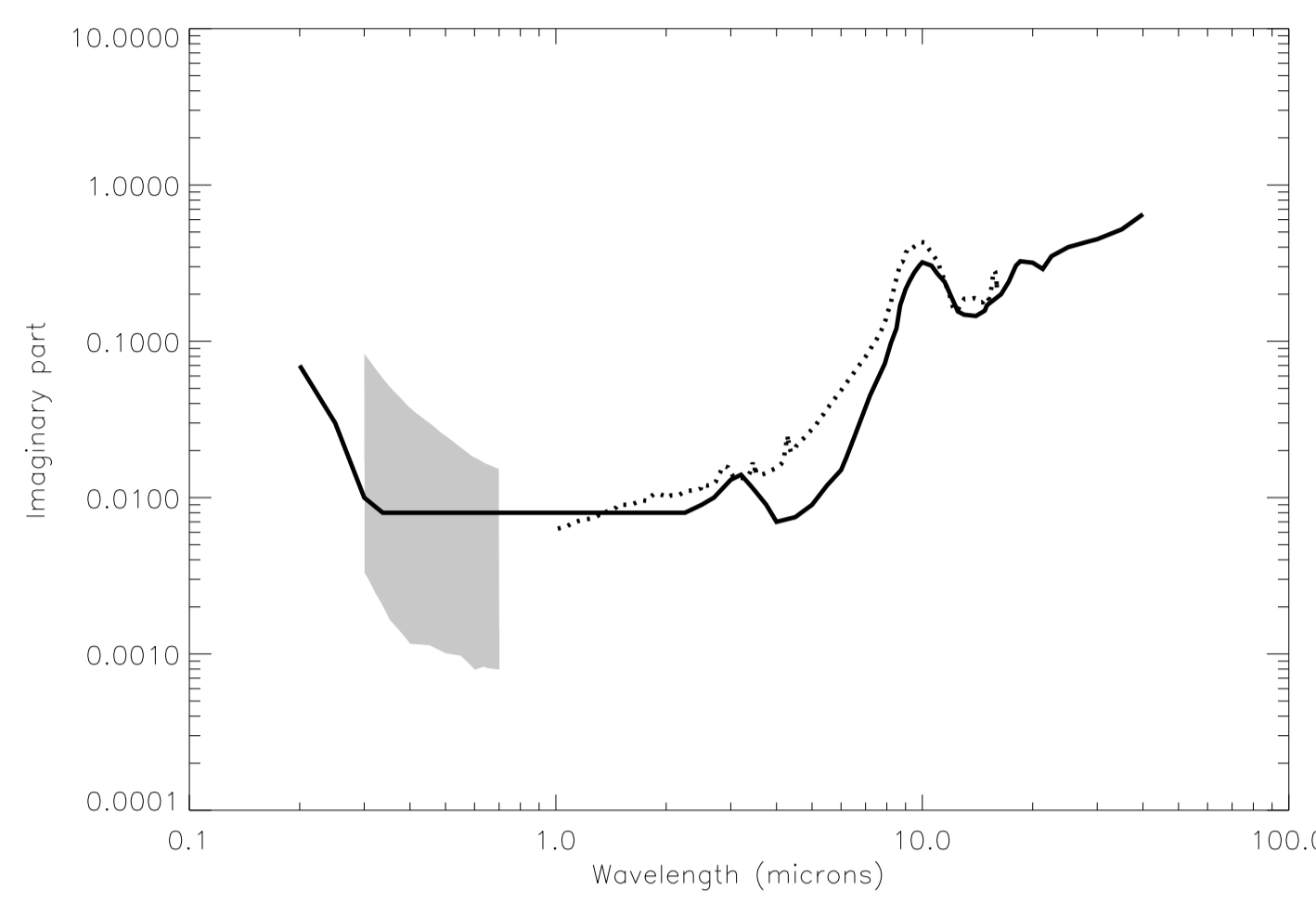


Figure 3: Summary of the published imaginary refractive index of ash given in Table 1. The shaded area shows the range of published data. The dotted line shows the only available infrared data (Patterson [7]). For comparison the widely used pumice data from Volz [11] is plotted.

Table 2, and Figures 4 and 5 show the data that has commonly been used in the atmospheric literature for ash refractive index's. These are in-fact not refractive index of Ash's but "ash-like" substances. This data shows the large range of imaginary refractive index reported (shaded area in plots).

Table 2: Published refractive index data for ash like material.

Material	SiO ₂ wt. %	Spectral range (μm)	n and k	Reference
Basaltic glass	53.45	0.5-50	n, k	[8]
Basalt	53.25	0.5-50	n, k	[8]
Basalt	51.45	0.2-0.4	n, k	[1]
Andesite	54.15	0.5-50	n, k	[8]
Andesite	55.10	0.2-0.4	n, k	[1]
Pumice	-	2.5-40	n, k	[11]
Granite	71.30	5-40	n, k	[10]
Obsidian	73.45	0.5-50	n, k	[8]
Obsidian	76.20	0.5-50	n, k	[8]

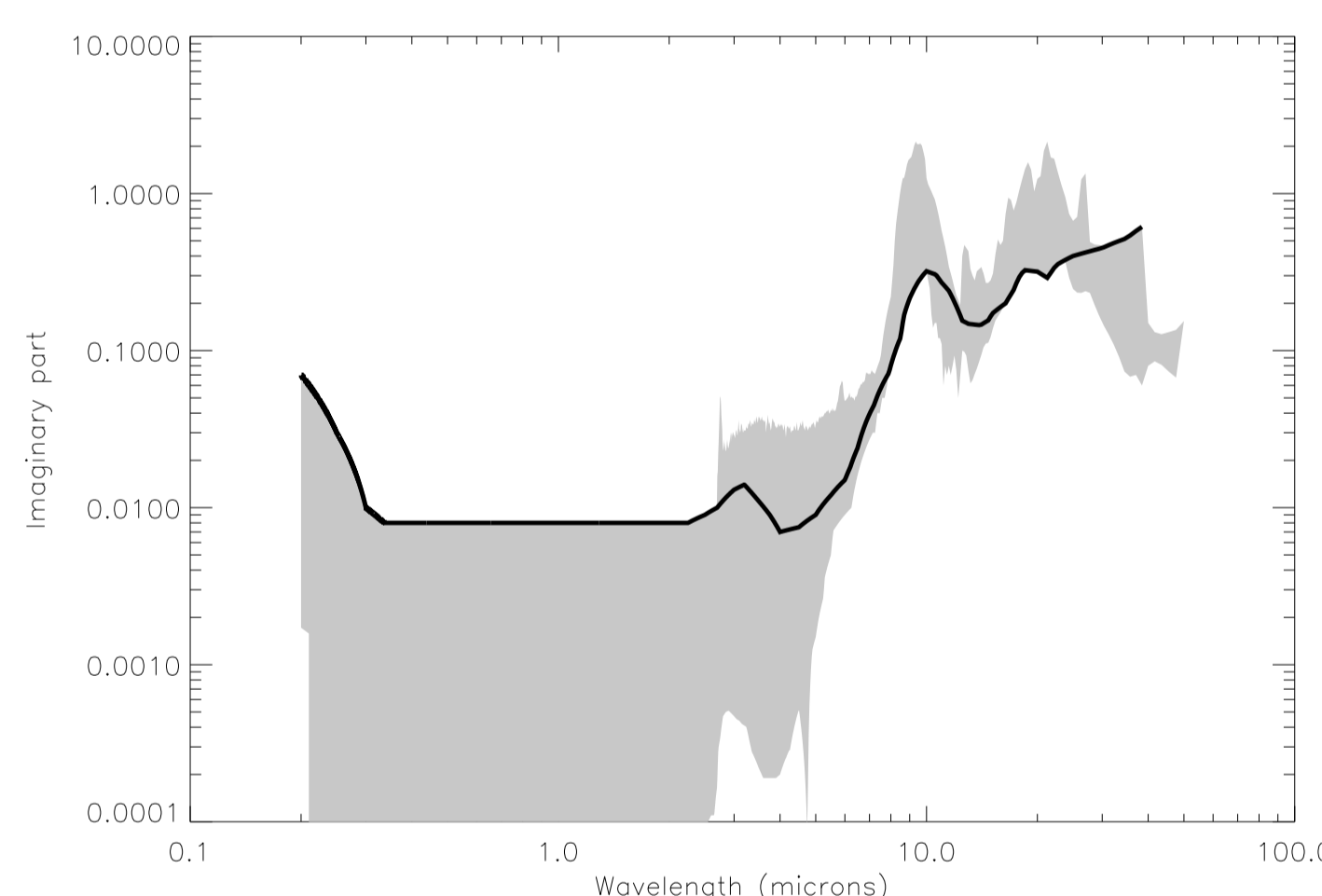


Figure 4: Summary of the published imaginary part of volcanic ash like refractive index. Shaded area shows the range of published data. The solid line shows the widely used pumice data from Volz (1973) [11].

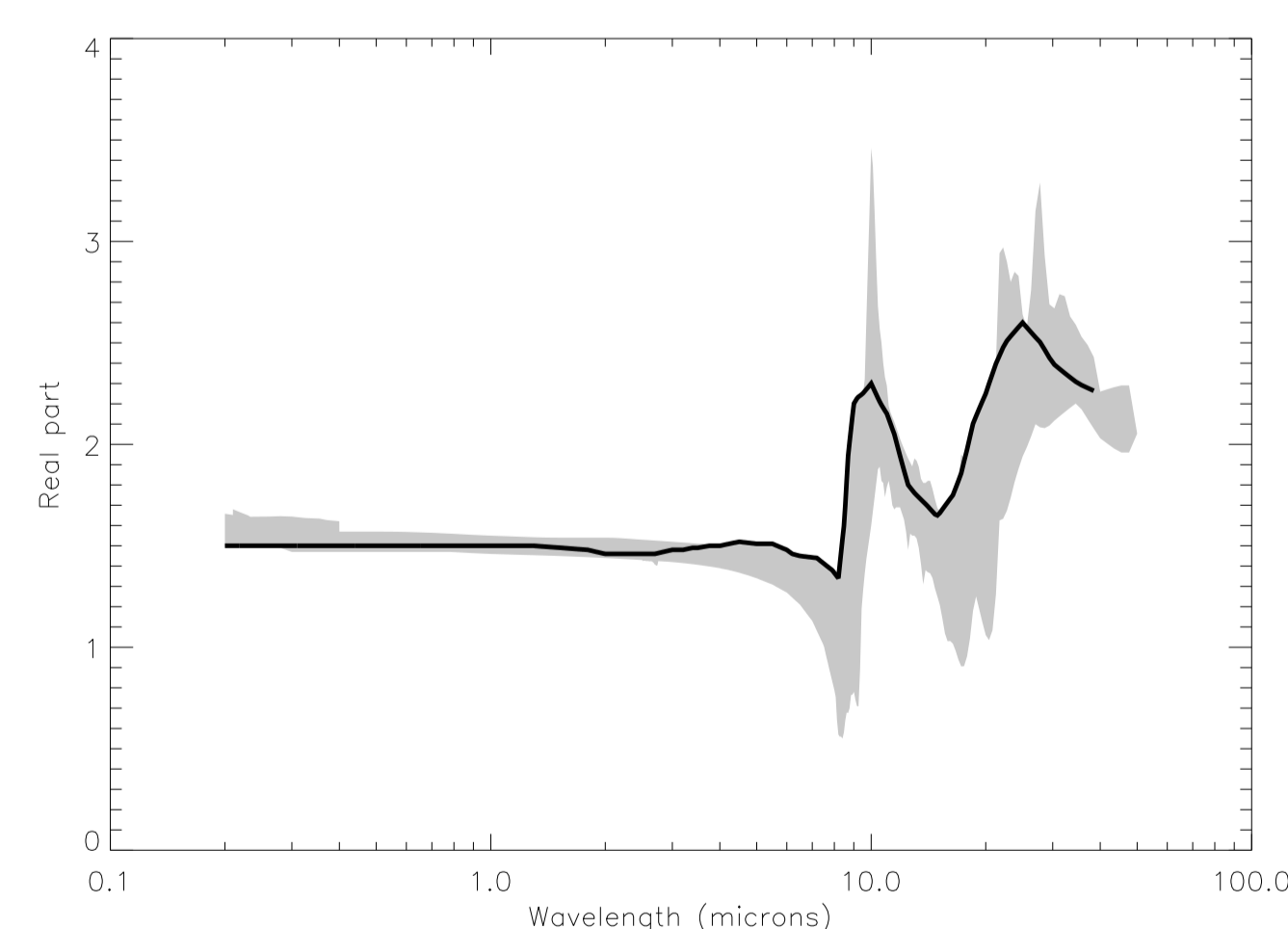


Figure 5: Summary of the published real part of volcanic ash like refractive index. Shaded area shows the range of published data. The solid line shows the widely used pumice data from Volz [11].

4 New measurements

To improve our knowledge of ash refractive index's this project takes measurements of the optical properties in the laboratory. The method used is described in Thomas [9]. This method inverts for refractive index from measurements of optical transmission of a suspended aerosol. As part of this project a new multi-pass cell has been commissioned to increase signal to noise ratio of the measurements. Initial results are shown in Figure 6. Figure 7 shows retrieved refractive index data from earlier single pass cell measurements.

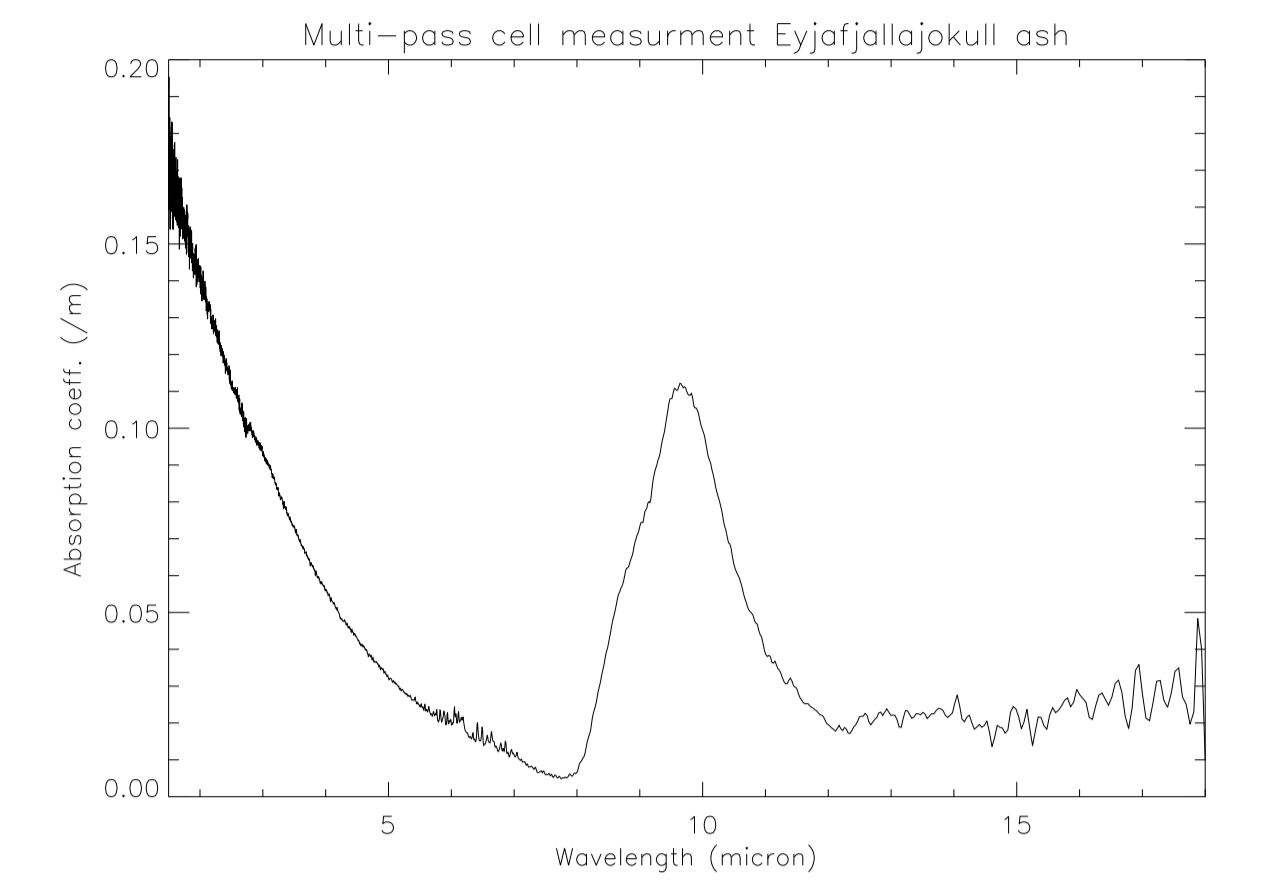


Figure 6: Multi-pass cell initial testing.

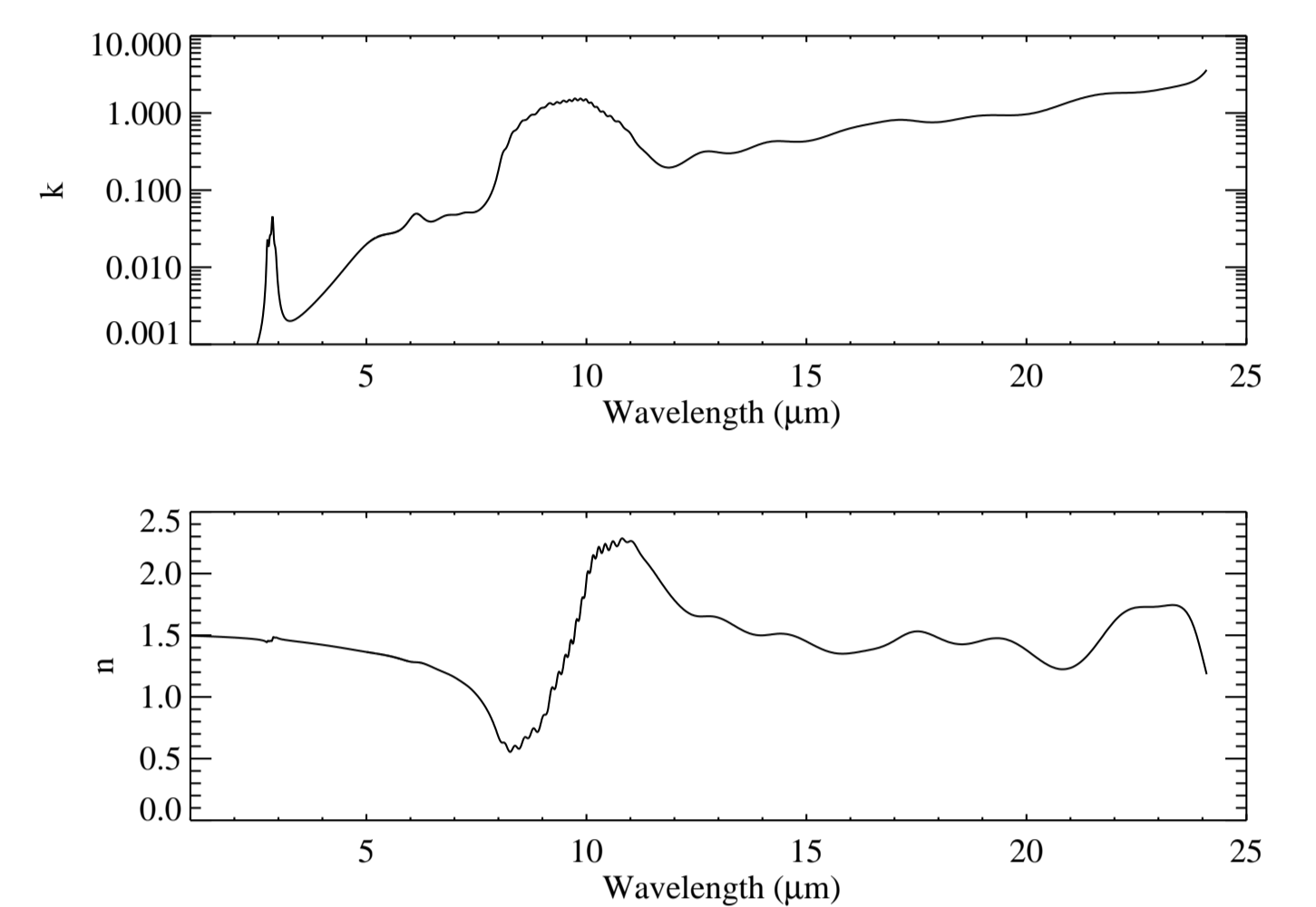


Figure 7: Single pass cell example results for Aso ash.

5 Independent data

To help verify the retrieved refractive index, additional independent measurements of refractive index is required. Measurements have recently been taken on our ash samples using the standard Becke Line method. Results are shown in Table 3, and example microscopy are shown in Figures 8 and 9.

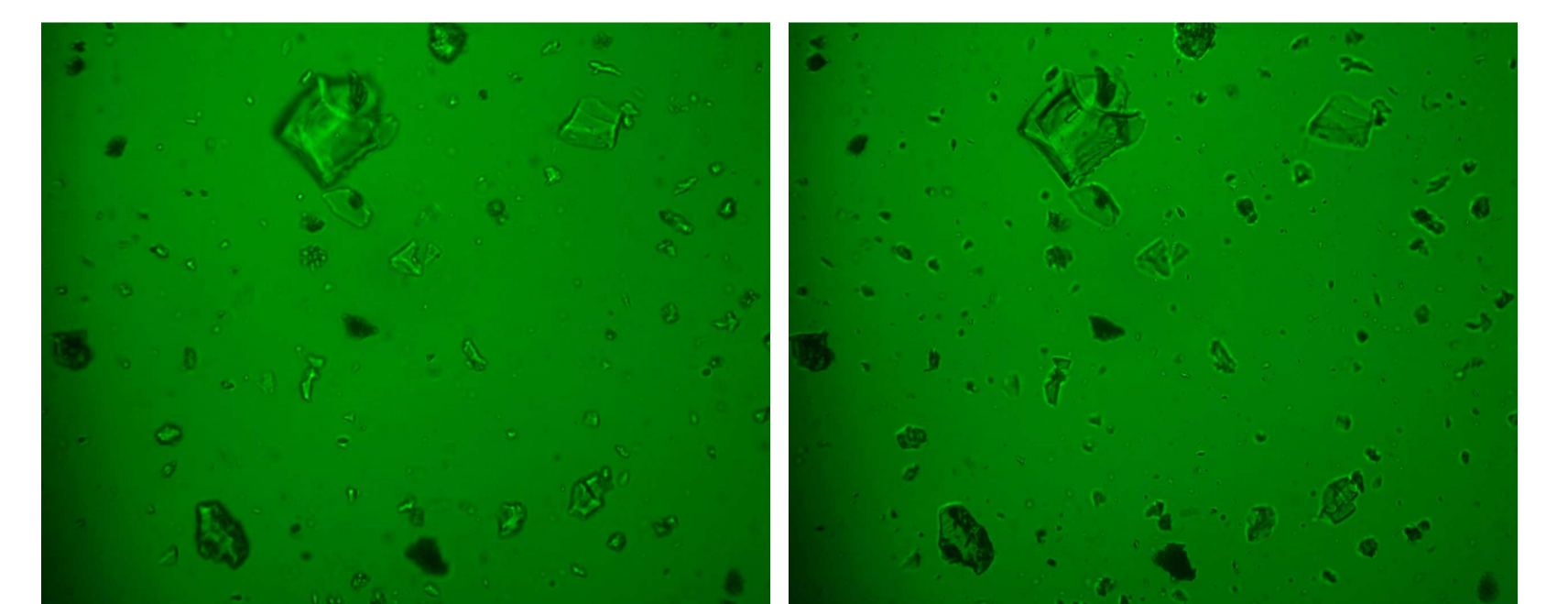


Figure 8: Eyjafjallajökull ash in 1.60 refractive index liquid with 546 nm filter. From left to right panel the objective lens is raised and the Becke Line is seen to move out of the particles, indicating that the liquid has a higher refractive index. The frame is approximately $400 \mu\text{m}$ across.

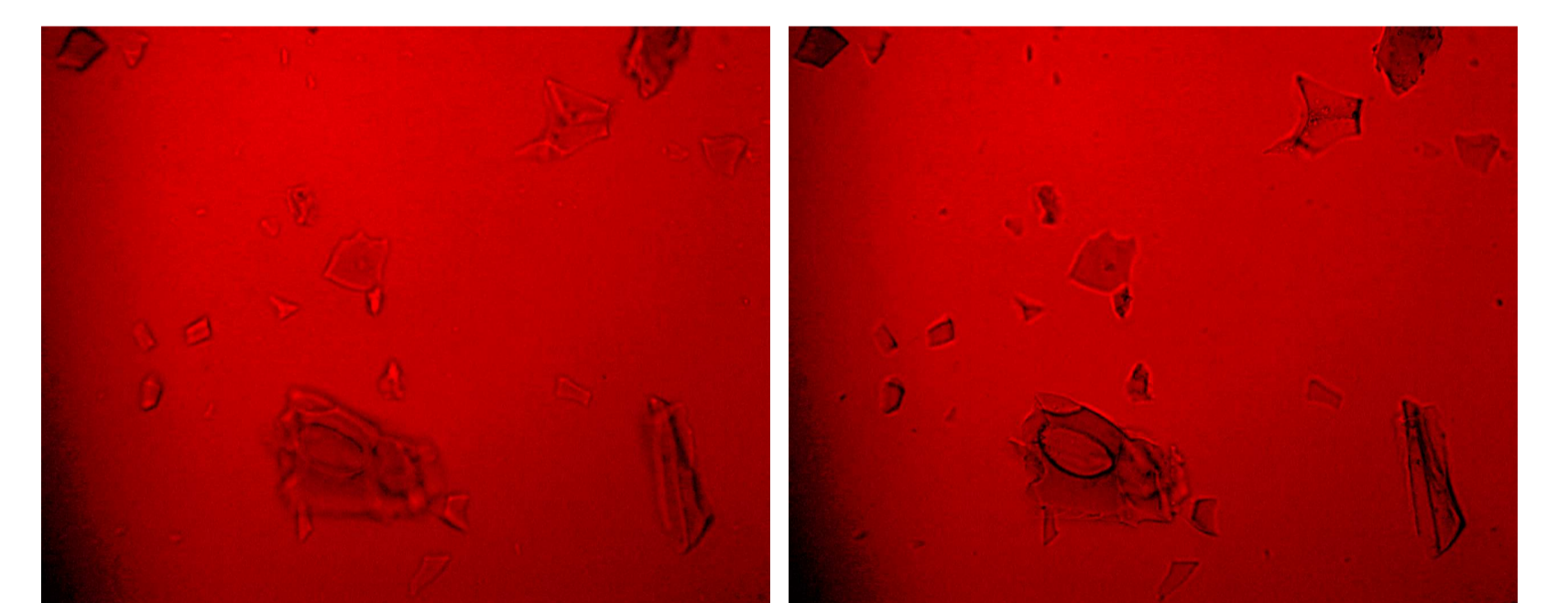


Figure 9: Grímsvötn Ash in 1.65 refractive index liquid with 650 nm filter. From the left to right panel the objective lens is raised and the Becke Line is seen to move out of the particles, indicating that the liquid has a higher refractive index than the fragments.

Table 3: Results for Becke Line mean particle refractive index.

Ash Sample	Mean Particle Refractive Index, $n_p(\lambda)$		
	450.0 nm	546.1 nm	650.0 nm
Mt Aso Volcanic Ash	1.577	1.562	1.553
Grímsvötn Volcanic Ash - May 2011	1.629	1.608	1.597
Grímsvötn Volcanic Ash - June 2011	1.623	1.608	1.596
Eyjafjallajökull	1.572	1.562	1.554
Etna E2	1.605	1.593	1.582
Afar Boina BA1	1.521	1.513	1.507
Afar Boina BA2	1.516	1.516	1.519
Etna December 2012		1.600	
Rhyolite Ash Chaiten	< 1.516	< 1.505	< 1.499

References

- [1] W. G. Egan, T. Hilgeman, and K. Pang. Ultraviolet complex refractive-index of Martian dust - laboratory measurements of terrestrial analogs. *Icarus*, 25(2):344-355, 1975.
- [2] G. M. Hale and M. R. Querry. Optical constants of water in the 200 nm to 200 μm wavelength region. *Applied Optics*, 12:555-563, 1973.
- [3] N. A. Krotkov, D. E. Filtner, A. J. Krueger, A. Kostinski, C. Riley, W. Rose, and O. Torres. Effect of particle non-sphericity on satellite monitoring of drifting volcanic ash clouds. *Journal of Quantitative Spectroscopy and Radiative Transfer*, 63:613-630, 1999.
- [4] B. Luo, U. K. Krieger, and T. Peter. Densities and refractive indices of $\text{H}_2\text{SO}_4/\text{HNO}_3/\text{H}_2\text{O}$ solutions to stratospheric temperatures. *Geophysical Research Letters*, 23(25):3707-3710, 1996.
- [5] E. M. Patterson. Measurements of the imaginary part of the refractive index between 300 and 700 nanometers for moist st. helens ash. *Science*, 1981.
- [6] E. M. Patterson, C. O. Pollard, and I. Galindo. Optical-properties of the ashes from El-Chichón volcano. *Geophysical Research Letters*, 10(4):317-320, 1983.
- [7] Edward M. Patterson. Optical absorption coefficients of soil-aerosol particles and volcanic ash between 1 and 16 μm . In *Second Conference on Atmospheric Radiation (American Meteorological Society)*, pages 177-180, 1975.
- [8] J. B. Pollack, O. B. Toon, and B. N. Kare. Optical properties of some terrestrial rocks and glasses. *Icarus*, 19(3):372-389, 1973.
- [9] Gareth E. Thomas, Stephen F. Bass, Roy G. Grainger, and Alyn Lambert. Retrieval of aerosol refractive index from extinction spectra with a damped harmonic-oscillator band model. *Applied Optics*, 2005.
- [10] O. B. Toon, J. B. Pollack, and C. Sagan. Physical properties of the particles composing the martian dust storm. *Icarus*, 30:663-696, 1977.
- [11] Frederic E. Volz. Infrared optical constants of ammonium sulfate, sahara dust, volcanic pumice, and flyash. *Applied Optics*, 12(3):564-568, March 1973.
- [12] S. G. Warren and R. E. Brandt. Optical constants of ice from the ultraviolet to the microwave: A revised compilation. *Journal of Geophysical Research*, 113(D14):D14220, 2008.